Cell Calcium 105 (2022) 102605

Contents lists available at ScienceDirect

Cell Calcium

journal homepage: www.elsevier.com/locate/ceca

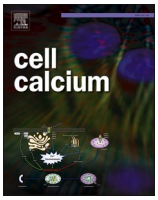

STIM1 and ORAI1 mutations leading to tubular aggregate myopathies are sensitive to the Store-operated Ca^{2+}-entry modulators CIC-37 and CIC-39

Beatrice Riva [a], Emanuela Pessolano [a], Edoardo Quaglia [a], Celia Cordero-Sanchez [a], Irene P. Bhela [a], Ana Topf [b], Marta Serafini [a,1], Daniel Cox [b], Elizabeth Harris [b], Matteo Garibaldi [d], Rita Barresi [c], Tracey Pirali [a], Armando A. Genazzani [a,*]

[a] Department of Pharmaceutical Sciences, Università del Piemonte Orientale, Italy
[b] John Walton Muscular Dystrophy Research Centre, Faculty of Medical Sciences, Translational & Clinical Research Institute, Newcastle University, Newcastle upon Tyne, UK
[c] IRCCS San Camillo Hospital, Venice, Italy
[d] Dipartimento di Neuroscienze, Salute Mentale e Organi di Senso (NESMOS), SAPIENZA Università di Roma, Italy

ARTICLE INFO

Keywords:
Store-operated calcium entry
Tubular aggregate myopathy
Gain-of-function mutation
Store-operated calcium entry modulators

ABSTRACT

Gain-of-function mutations on STIM1 and ORAI1 genes are responsible for an increased store-operated calcium entry, and underlie the characteristic symptoms of three overlapping ultra-rare genetic disorders (*i.e* tubular aggregate myopathy, Stormorken syndrome, York platelet syndrome) that can be grouped as tubular aggregate myopathies. These mutations lead to a wide spectrum of defects, which usually include muscle weakness and cramps.

Negative modulators of store-operated Ca^{2+}-entry targeting wild-type STIM1 and ORAI1 have entered clinical trials for a different array of disorders, including pancreatitis, COVID-19, cancer, and autoimmune disorders and, while efficacy data is awaited, safety data indicates tolerability of this

STIM1/ORAI1 mutations are amenable to pharmacological intervention. If this were so, given that there are no approved treatments or clinical trials ongoing for these rare disorders, it could be envisaged that these agents could also rehabilitate tubular aggregate myopathy patients. In the present contribution we characterized the Ca^{2+}-entry patterns induced by eleven STIM1 and three ORAI1 mutations in heterologous systems or in patient-derived cells, *i.e.* fibroblasts and myotubes, and evaluated the effect of CIC-37 and CIC-39, two novel store-operated calcium entry modulators. Our data show that all STIM1 and ORAI1 gain-of-function mutations tested, with the possible exception of the R304Q STIM1 mutation, are amenable to inhibition, albeit with slightly different sensitivities, paving the way to the development of SOCE modulators in tubular aggregate myopathies.

1. Introduction

Tubular aggregate myopathies (TAM) are ultrarare genetic disorders characterized histologically by tubular aggregates in skeletal muscle that can be observed by electron microscopy [1,2]. From a clinical perspective, muscle weakness and cramps are usually present, although the disorder can manifest itself as a multisystemic syndrome that, among other features, presents thrombocytopenia [3]. The classical multi-systemic disorder is also known as Stormorken syndrome [4–6] while the disease that is predominantly characterized by thrombocytopenia is known as York Syndrome [7].

These disorders arise from an abnormal store-operated calcium entry (SOCE), *i.e.* the mechanism by which cells sense a decrease in luminal Ca^{2+} in the endoplasmic reticulum (ER) and trigger its replenishment by inducing Ca^{2+}-entry across the plasma membrane [8]. TAM arises from gain-of-function mutations in the genes encoding for the two main players in SOCE: ORAI1, the Ca^{2+}-channel that resides on the plasma membrane, or STIM1, the calcium sensor within the ER that upon store

Abbreviations: TAM, tubular aggregate myopathy; SOCE, store-operated calcium entry; ER, endoplasmic reticulum; STIM, stromal interaction molecule; ORAI, calcium release-activated calcium channel protein; SAM, sterile alpha-motif.

* Corresponding author.
E-mail address: armando.genazzani@uniupo.it (A.A. Genazzani).
[1] Present address: Department of Chemistry, Chemistry Research Laboratory, University of Oxford, 12 Mansfield Road, OX1 3TA, UK

https://doi.org/10.1016/j.ceca.2022.102605
Received 7 January 2022; Received in revised form 9 April 2022; Accepted 16 May 2022
Available online 18 May 2022

depletion directly triggers ORAI1 opening [9]. More recently, mutations in calsequestrin, an ER Ca^{2+}-buffering protein, have also been associated with cases of TAM [10,11]. As depicted in Fig. 1, numerous mutations on either ORAI1 or STIM1 have been associated to TAM. Most reported mutations on ORAI1 reside in the first transmembrane domain, although gain-of-function mutations in all transmembrane domains have been reported [1,12]. Regarding STIM1, most reported mutations, albeit mostly in single families, are located in the canonical and non-canonical EF hand domains that sense intraluminal Ca^{2+}, and this has been shown to lead to constitutive oligomerization and activation of SOCE [1,13]. A mutation on the sterile alpha-motif (SAM), also known to participate in protein-protein interactions, has been recently reported to lead to TAM in a single family [14]. Mutations in the cytosolic portion of the protein, where coiled-coil domains for protein-protein interactions are present, have a lower variety but the p.R304W is the most frequently reported mutation, with at least 13 families affected [15]. Again, constitutive oligomerization and SOCE activation were reported [16]. A recent review attempted to create a genotype/phenotype correlation of the disorder [13], but given the paucity of data, the results are difficult to interpret unambiguously. Briefly, mutations in the EF-hands motifs do not predict clinical severity (from asymptomatic to childhood-onset symptoms), R304W mutation leads to Stormorken syndrome [17], while ORAI1 mutations lead to childhood-onset symptoms [13].

Due to the involvement of SOCE in important cellular processes both in non-excitable and excitable cells, a number of different compounds have been developed that hamper Ca^{2+}-entry plausibly *via* binding to ORAI1. CM4620 is at present the most advanced SOCE inhibitor in clinical development, has completed Phase II studies for acute pancreatitis [18–22] and is also being investigated for other conditions, including COVID-19 [23–25]. SOCE inhibitors are also in Phase I and Phase I/Ib for the treatment of autoimmune disorders (RP3128, [26–28]) and for relapsed or refractory lymphomas (RP4010, [29]).

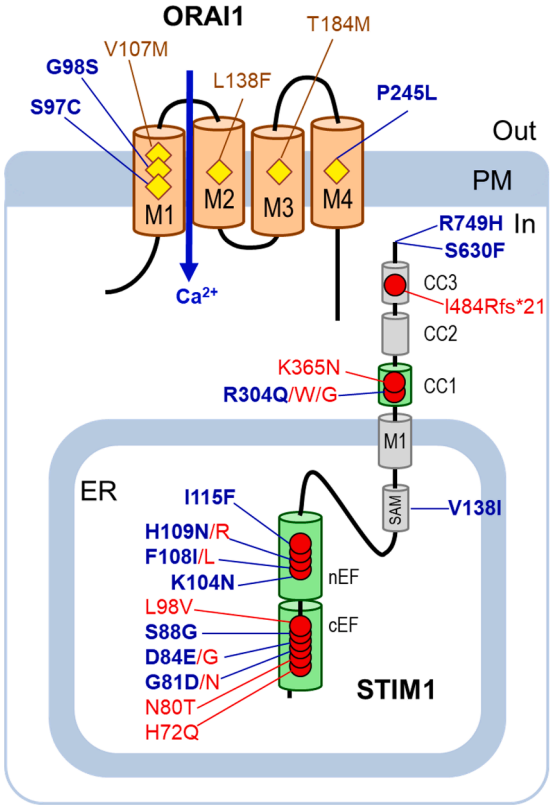

Figure 1. Gain-of-function mutations reported to lead to tubular aggregate myopathy in humans. In blue, the mutations used in the present contribution.

Overall, RP3128 has been shown to have good tolerability in humans [26,27], and reports on efficacy are eagerly awaited.

Alongside the above molecules, a number of groups are now reporting further molecules that affect SOCE [30–33]. Due to the ultra-rare nature of TAM, with just over 50 families reported in the literature [13], no specific drug program is, to our knowledge, active. Yet, one could speculate that SOCE inhibition could be an effective and convenient mean to counteract the gain-of-function effect of mutations, also in view of the tolerability shown by these agents in clinical trials for other disorders. Importantly, given that TAM may arise from a number of different mutations on ORAI1 or STIM1, the sensitivity of these natural mutations has been scarcely investigated in the literature and should be established. A few studies have concentrated on mutations designed to understand ORAI1 function or binding mode of specific inhibitors. Among the best characterized inhibitors of SOCE is 2-APB which according to the concentration can either facilitate or inhibit SOCE. These actions have been shown to be attributable both to a direct and indirect action on ORAI1 [34]. 2-APB has been shown to inhibit STIM1-independent currents when constitutively active ORAI1 mutants are used (p.P245T and p.V102A), while it loses its inhibitory activity on the p.V102C mutant. These data would suggest that disease-leading mutant ORAI1 channels can be pharmacologically inhibited. Similarly, Synta66, a specific SOCE inhibitor, that computational docking studies have suggested to bind to the extracellular loop 1 and 3 of ORAI1 is effective in some mutants [32], but loses activity in mutants around the selectivity filter (*e.g.* p.E106D). A similar effect of this mutation was observed more recently with the lead compound of a novel series of SOCE inhibitors [33]. While the above ORAI1 mutations were designed to gather insights on the binding mode of SOCE inhibitors, Bulla et al investigated natural TAM-associated mutations of ORAI1 to understand whether these could be amenable to pharmacological intervention [31]. The Authors found that the p.V107M, p.L138F, p.T184M and the p.P245L were all sensitive to GSK-7975A, a specific ORAI1 and ORAI3 inhibitor [35] that was shown to be effective in models of acute pancreatitis [36], while the p.G98S mutation was resistant to inhibition. Overall, the above observations indicate that SOCE inhibitors that bind to the ORAI1 channel are able to inhibit the activity of most mutated ORAI1 channels. To our knowledge, with the exception of the paper by Bulla et al. [31], no other natural mutations of ORAI1 have been investigated and the ability of SOCE inhibitors to modulate SOCE triggered by mutated STIM1 has so far not been investigated.

In the present contribution, we used heterologous systems to characterize the Ca^{2+}-entry patterns induced by different mutations and to establish the sensitivity of CIC-37 and CIC-39, two structurally-distinct, recently described, SOCE inhibitors. CIC-37 was developed starting from a class of pyrazole-bearing molecules that had micromolar activity [37] but also suffered from off-target effects on other channels and was proven to be selective compared to the parent compounds [38]. CIC-39 is a biphenyl-triazole and was designed starting from Synta66 [39], a chemical tool often used in cellular experiments to inhibit SOCE [40]. Both compounds were shown to be selective over other channels and were effective at reducing cerulein-induced pancreatitis in rodent models [38,40]. Overall, we conclude that TAM-leading mutations in cellular fluorimetry models of Ca^{2+}-signaling behave similarly and are mostly sensitive to CIC-37 and CIC-39. To confirm this, we also investigated patient-derived fibroblasts and myotubes and found similar results, with the exception of the R304Q mutation, which is less sensitive to inhibition by both CIC-37 and CIC-39. Our data therefore suggest that these compounds could be developed as therapeutic agents for most, albeit not all, genetic mutations leading to TAM.

2. Materials and methods

2.1. Cell culture

The use of human fibroblasts was approved by the Newcastle MRC

Centre Biobank for Neuromuscular Diseases (REC reference 19/NE/0028). Human fibroblasts and human embryonic kidney HEK cells (ATCC, Rockville, MD, USA) were cultured in Dulbecco's Modified Eagle's Medium (DMEM; Sigma-Aldrich, Italy), supplemented with 10% heat-inactivated Fetal Bovine Serum (FBS, Gibco, Italy), L-glutamine 50 mg/mL (Sigma-Aldrich, Italy), penicillin 10 U/mL and streptomycin 100 mg/mL (Sigma-Aldrich, Italy) at 37°C, under a 5% CO_2 humidified atmosphere. Human myoblasts were obtained and differentiated into myotubes as previously reported [41]. Informed consent was obtained from the patient and the research protocol for the use of the biopsy taken for diagnostic reasons was planned and carried out in accordance of the policies of Sapienza University.

For calcium imaging experiments, human fibroblasts and HEK cells were plated onto glass coverslips at concentrations of 15×10^4 and 5×10^4 *per* mL, respectively (24 mm diameter coverslips in 6 well plates), while, for differentiation in myotubes, human myoblasts were plated in DMEM with 10% heat-inactivated horse serum at a concentration of 20×10^4 per well. Experiments were performed 6-7days after myoblast isolation from muscle biopsy at cell passage number P2 and P3.

2.2. Mutagenesis and generation of STIM1/ORAI1 mutated HEK cells

The pMAX-RFP plasmids carrying the cDNA for STIM1 and ORAI1 were obtained from a collaborating group (Barbara Niemayer; Saarland University; Homburg).

The STIM1 (c.252T>A p.D84E; c.312A>T p.K104N; c.322T>A p.F108I; c.326A>G p.H109R; c.343A>T p.I115F c.412G>A p.V138I; c.1889C>T p.S630F; c.2246G>A p.R749H) and ORAI1 (c.290C>G p.S97C; c.292G>A p.G98S; c.734C>T p.P245L) mutants were created by exchanging the corresponding codons using QuikChange lighting site directed mutagenesis kit (Agilent, USA) and specific primers. The list of primers used is reported in Supplementary Table1 and 2. PCR products were controlled by Sanger LIGHTrun sequencing from Microsynth AG (Switzerland). For cell transfection, 7 μg of each plasmid DNA were transfected using lipid reagent lipofectamine (Lipofectamine 2000 Transfection Reagent, Life Technologies). Twenty-four hours after transfection, PCR was performed to evaluate the gene expression.

2.3. Real time quantitative PCR (qRT-PCR)

Total RNA isolation and qRT-PCR were performed as previously reported [42]. Primers used are listed in Supplementary Table 3.

2.4. Western blot analysis

HEK cells were lysed in RIPA buffer. Lysates were clarified by centrifugation at 14,000 g for 15 min at 4°C and 20 μg of protein from each sample were loaded on SDS-PAGE gels. STIM1 (4916 Cell signalling) was prepared in 5% bovine serum albumin in TRIS-buffered saline solution containing 0.1% Tween-20 (T-TBS) while ORAI1 (PA-74181, Invitrogen) ws prepared in 3% non-fat dried milk in TRIS-buffered saline solution containing 0.1% Tween-20 (T-TBS), according to the manufacturer instructions.

2.5. Fura-2 Ca^{2+} measurements

Cells were loaded with 5 μM Fura-2 AM in the presence of 0.02% of Pluronic-127 (both from Life Technologies, Italy) and 10 μM sulfinpyrazone (Sigma Aldrich, Italy) in Krebs–Ringer buffer (KRB, 135 mM NaCl, 5 mM KCl, 0.4 mM KH_2PO_4, 1 mM $MgSO_4$, 5.5 mM glucose, 20 mM HEPES, pH 7.4) containing 2 mM $CaCl_2$ (30 min, room temperature) on poly-L-lysine (P4832, Sigma Aldrich) coated glass coverslips. Basal calcium and SOCE measurements were performed as stated elsewhere [38,42]. For those experiments in which a Ca^{2+}-calibration was performed, at the end of each recording, HEK cells were perfused with a solution containing 10 μM ionomycin with either 10 mM Ca^{2+} or 25 mM EGTA. Concentrations of Ca^{2+} were calculated according to Grynkiewicz et al. [43].For Mn^{2+} quenching assays, cells were treated for 10 min with 50 μM *t*BHQin a Ca^{2+}-free KRB solution containing 500 μM to induce ER release. Thereafter, 500 μM Mn^{2+} was added. After 300 s SOCE activation was evaluated considering the decay slope in the presence or absence of selected compounds (CIC-37 and CIC-39).

2.6. Statistical analysis

Data are presented as mean ± SEM or median and interquartile range (IQR). The normality of data distributions was assessed using the Shapiro−Wilk test. Parametric (Student t-test) or nonparametric (Mann-Whitney U test) statistical analyses were used for comparisons of data. All statistical assessments were two-sided and a value of $P < 0.05$ was considered statistically significant. Statistical analyses were performed using GraphPad Prism software (GraphPad Software, Inc., USA).

3. Results

3.1. *ORAI1 and STIM1 mutations associated to TAM lead to an increased* $[Ca^{2+}]_{basal}$ *and an increased SOCE in HEK cells*

Of the mutations reported to lead to TAM (Fig. 1), the p.F108I and p.I115F mutations on STIM1 have not been previously characterized for cellular Ca^{2+} signalling changes, although their clinical consequences have been reported [1,3,44]. We therefore generated these sequences by mutagenesis and complemented the collection with other mutations to cover other protein regions on the two incriminated proteins (in blue in Fig. 1). We also chose the ORAI1 p.G98S and p.P245L mutations to bridge our findings with those obtained by Bulla et al. on GSK-7975A [31]. Some important mutations, such as the R304Q on STIM1, were not generated as the lab also had access to some patient-derived fibroblasts or myotubes bearing these mutations (see below). To characterize the impact of these mutations on Ca^{2+}-signalling, we took advantage of the dominant nature of the disorder and therefore transiently transfected wild-type HEK cells. To control for the increased protein due to the transfection, control cells were transfected with either the wild-type STIM1 or ORAI1 gene. When evaluating mRNA levels in the different cell lines by real-time PCR (Supplementary Fig. 1A), transfected cells showed a significant increase over untransfected cells, but no significant differences were observed between mutants and transfected control cells. Regarding the protein levels, all STIM1 transfected cells showed a STIM1 expression significantly increased as compared to un-transfected cells (HEK WT). The p.D84E and p.K104N mutants surprisingly revealed an increased level also compared to control transfected cells (HEK STIM1 Ctrl, Supplementary Fig. 1B upper panel). Such increase, surprisingly, was reflected also in the ORAI1 protein. Transfected cells with the ORAI1 constructs showed an increased ORAI1 protein compared to untrasfected cells, while no difference was observable between control and mutant proteins.

We next proceeded to evaluate $[Ca^{2+}]_{basal}$ and the presence of oscillations, as changes in this have been reported previously for other mutations in patient derived cells [3,17,41,45,46]. As it can be observed in Fig. 2A, all STIM1 and ORAI1 mutants led to a significantly increased $[Ca^{2+}]_{basal}$, although the level of this increase was variable. In HEK cells, no oscillations were evident with any of the mutants when observing untreated cells for 10 min (not shown).

We next proceeded to evaluate Ca^{2+-}entry triggered by store depletion. Briefly, cells were depleted of intracellular Ca^{2+} by incubating them with the SERCA poison *t*BHQfor 10 min and then Ca^{2+} was re-added. As it can be observed, in wild-type HEK cells this re-addition triggered an expected cytosolic Ca^{2+}-rise, which corresponds to SOCE. Transfection of cells with wild-type STIM1 or wild-type ORAI1 led to a greater Ca^{2+} entry, possibly due to an increased protein level. Importantly, though, cells bearing the p.F108I and p.I115F mutations on STIM1 showed a significantly higher level of Ca^{2+}-entry, compared to

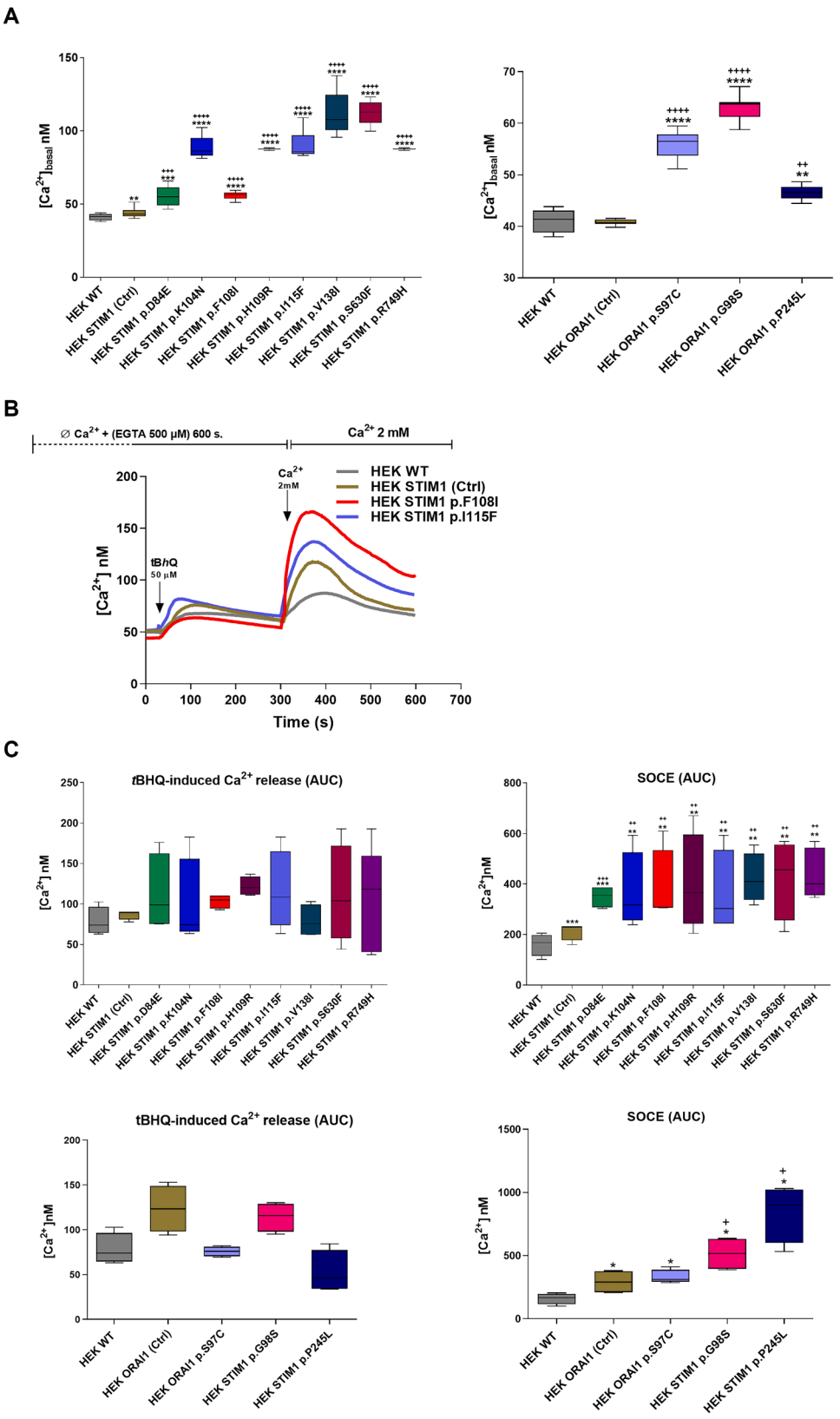

Figure 2. Evaluation of $[Ca^{2+}]_{basal}$ and SOCE. (**A**) Average $[Ca^{2+}]_{basal}$ in cells transfected with the indicated mutations, transfected with the wild-type (Ctrl) STIM1/ORAI1 sequences or un-transfected (WT). Box and whisker plots show median and IQR of $[Ca^{2+}]_{basal}$. Mann-Whitney U test. $[Ca^{2+}]_{basal}$ **** $P<0.0001$ *vs* HEK WT; $^{\#\#\#\#}\leq P0.0001$ *vs* HEK STIM1 (Ctrl) or HEK ORAI1 (Ctrl). (**B**) SOCE triggered by re-addition of extracellular Ca^{2+} after *t*BHQ-induced store depletion in cells transfected with the indicated mutants. Average Ca^{2+}-traces of approximately 200 cells from eight separate coverslips performed on 2 separate days. (**C**) Area under the curve (AUC) of SOCE in cells transfected with the indicated mutations, with the wild-type (Ctrl) STIM1/ORAI1 sequences, or un-transfected (WT). For tBHQ-induced Ca^{2+}-release, AUC was quantified for 270 s (from second 30 to second 300). For SOCE, AUC was quantified for 300 s (from second 300 to second 600).

Box and whisker plots show median and IQR of the AUC. AUC *P= 0.046, **P ≤0.043, ***P=0.001 vs HEK WT; $^{++}P\leq 0.025$ vs HEK STIM1(Ctrl), $^{+}P=0.048$ vs HEK ORAI1 (Ctrl).

their respective controls, thereby confirming the gain-of-function nature of these previously uncharacterized mutations (Fig. 2B), and providing a cellular correlate to the clinical phenotype [44]. As expected, a similar effect was observed with all other STIM1 and ORAI1 mutations that were quite similar in behavior, although p.H109R, p.V138I, p.S630F, and R749H displayed a greater effect among STIM1 mutations, while the p.G98S mutation exhibited the most pronounced effect among ORAI1 mutations (Supplementary Fig. 2A).We also evaluated the store depletion phase due to *t*BHQtreatment and found that the amount of stored Ca^{2+}, as determined by -induced release, was not significantly modified.

All these evidences are supported by the parameters evaluated (area under the curve, peak amplitude and slope, Fig. 2C and D; Supplementary Fig. 2C-E). Given the heterologous nature of this model, the uncontrolled protein levels and the non-systematic nature of clinical data reporting for individual families, we did not attempt to correlate the Ca^{2+}-differences between mutations with any clinical repercussion.

3.2. STIM1 and ORAI1 gain-of-function mutations are sensitive to SOCE modulators

We next tested whether this aberrant increase of Ca^{2+} triggered by mutations could be sensitive to the SOCE modulators we have previously described as effective on wild-type systems [38,40]. CIC-37 was tested at a concentration of 10 μM, that in our hand inhibits wild-type SOCE by 82.5±1.6 % (IC_{50}= 4.4 ± 1.2 μM) in HEK cells, while CIC-39 was tested at a concentration of 3 μM, that inhibits SOCE by 96.5 ± 2.4 % (IC_{50}= 851±54 nM). As shown in Table 1 and Supplementary Figs. 3 and 4, all STIM1 and ORAI1 mutations tested in HEK cells were sensitive to inhibition by these compounds, although with some slight differences. It should be noticed that the recently described p.V138I mutation, the mutation that responds with the least potency, is the only known STIM1 mutation in the SAM domain, setting it apart from all other mutations, located either in the intraluminal EF hands or in the cytosolic coiled-coil domains. Independently of the differences, the two compounds at the concentrations tested inhibited more than 50% of SOCE in all mutations.

Furthermore, it is important to note that, unlike previous data reported in the literature which revealed that the ORAI1 p.G98S mutation is completely resistant to GSK-7975A [31], we demonstrated that this mutation was sensitive to both tested compounds, even if the compounds showed a slightly decreased potency compared to other mutations.

Last, to further support these data, we performed Mn^{2+}-quench experiments in the presence or absence of the selected compounds. Briefly, cells were treated with *t*BHQ for 10 min and Mn^{2+} (500 μM) was added. The activation of SOCE was evaluated considering the decay slope of Fura-2 fluorescence upon Mn^{2+} addition and, as reported in Supplementary Fig. 5, un-transfected HEK cells (HEK WT) treated with CIC-37 and CIC-39 exhibited an abolishment of the quench, demonstrating the inhibitory effect of the selected compounds. The same experiments were also performed in HEK cells transfected with mutants and, accordingly Mn^{2+} quench was sensitive to inhibition by CIC-37 and CIC-39 (data not shown), in accord to Table 1 and Fura-2 measurements.

Table 1
SOCE inhibition by CIC-39 and CIC-37 in HEK cells transfected with STIM1/ORAI1 mutants.

GoF Mutations	SOCE Inhibition %(CIC-37 10 μM)	SOCE Inhibition %(CIC-39 3 μM)
STIM1p.D84E	70.9 ± 8.1	93.8 ± 2.2
STIM1 p. K104N	89.3 ± 2.6	91.4 ± 2.9
STIM1 p.F108I	70.5 ± 2.2	81.7 ± 3.3
STIM1 p. H109R	75.1 ± 7.3	82.7 ± 2.3
STIM1 p.I115F	90.9 ± 2.2	82.5 ± 3.5
STIM1 p.V138I	71.2 ± 7.3	62.8 ± 6.2
STIM1 p.S630F	83.4 ± 7.2	85.9 ± 2.2
STIM1 p. R749H	82.1 ± 6.5	92.9 ± 6.9
ORAI1 p. P245L	98.1 ± 3.5	98.2 ± 2.3
ORAI1 p.G98S	67.4 ± 6.1	76.6 ± 6.6
ORAI1 p.S97C	81.4 ± 7.3	78.7 ± 4.6

Values represent the % inhibition of the area under the curve (AUC) ± S.E.M.

3.3. Patient derived cells are also sensitive to SOCE modulators, with the exception of the R304Q mutation

Having established that natural gain-of-function mutations are broadly sensitive to SOCE modulators, we turned our attention to cells from affected individuals to establish whether contextualized mutations could also be druggable. In this respect, we had availability of fibroblasts harbouring p.G81D, p.S88G and p.R304Q STIM1 mutations (reported in [44]) and of myotubes derived from an Italian family harbouring the p.S97C ORAI1 mutation (reported in [41]). The p.G81D and p.S88G mutations are located in the EF-hand Ca^{2+}-binding motifs, and presumably affect the affinity for Ca^{2+} ions. The p.R304Q mutation is instead localized on the cytosolic coiled-coil domain of STIM1, presumably affects dimerization and resting state of the protein [15,44], and leads to the classical Stormorken syndrome.

We first investigated gene expression of the main SOCE components (STIM1, STIM2, ORAI1, ORAI2 and ORAI3) by qRT-PCR. Overall, mutated fibroblasts showed a slight, but significant, increase in STIM1 in comparison to fibroblasts harbouring wild-type STIM1 (Fig. 3A). These data suggest that these mutations do not significantly affect transcription of SOCE genes, in accord with other STIM1 and ORAI1 gain-of-function mutations previously described [1]. Next, we evaluated Ca^{2+}-signalling in these fibroblasts. We first monitored for 10 min fibroblasts cultured in a Ca^{2+}-containing solution without any stimulation. As it can be observed in Fig. 3B, $[Ca^{2+}]_{basal}$ in fibroblasts from affected patients was significantly higher compared to control fibroblasts. Furthermore, while $[Ca^{2+}]_{basal}$ in WT fibroblasts was stable (0/80 cells showed oscillations), most cells harbouring the p.G81D, p.S88G or p.R304Q mutations (78/80, 71/80 and 68/80, respectively) showed oscillations, which were slightly different in terms of frequency and intensity depending on the mutation (Fig. 3B). Oscillations have been reported previously in patient-derived cells, although not by all Authors [3,17,41,45]. We next analysed SOCE in these cells with the protocol described above, *i.e.* incubation of cells in *t*BHQ for 10 min and re-addition of extracellular Ca^{2+}. As it can be seen in Fig. 3C, all mutations induced a potentiation in SOCE. This was supported by all statistical parameters evaluated (maximum peak, slope and area under curve (AUC), Fig. 3D). Last, we primed the effect of the two inhibitors on these fibroblasts. In accordance with the effect on heterologous systems, both mutations residing on the EF hand motifs were sensitive to inhibition (Table 2, Fig. 4A,B). Yet, to some surprise, the R304Q mutation residing on the first coiled-coil motif, which gives rise to the archetypical Stormorken syndrome [15], was significantly less sensitive, with less than 40 % inhibition induced by CIC-39 (Fig. 4C; Table 2) and less than 20% inhibition by CIC-37.

We have previously characterized the effect of the p.S97C ORAI1 mutation in patient-derived myotubes. Briefly, as for the mutations above, myotubes harbouring the mutation show an increased $[Ca^{2+}]_{basal}$, oscillations and an enhanced SOCE [41]. Given the scarcity of the tissue, we could only test a single agent on these myotubes, and, as depicted in Fig. 5A and 5B, CIC-37 (3 μM) effectively mitigated SOCE overactivation also in p.S97C myotubes, restoring Ca^{2+} to a level similar to what observed in ORAI1 wild-type myotubes, while the concentration of 10 μM completely blocked SOCE (Supplementary Fig. 6). This is in accord to the effect of the two inhibitors on the ORAI1 p.S97C mutation in heterologous systems.

4. Discussion and conclusion

In the present contribution, we have characterized by fluorescence microscopy the Ca^{2+}-signalling changes occurring in cells harbouring STIM1 or ORAI1 mutations known to lead to TAM. For this, we used either a heterologous cellular system in which mutated genes were transfected in HEK cells or patient-derived fibroblasts and myotubes. The main difference observed in these two systems is the occurrence of spontaneous oscillations in contextualized cells, while in both systems

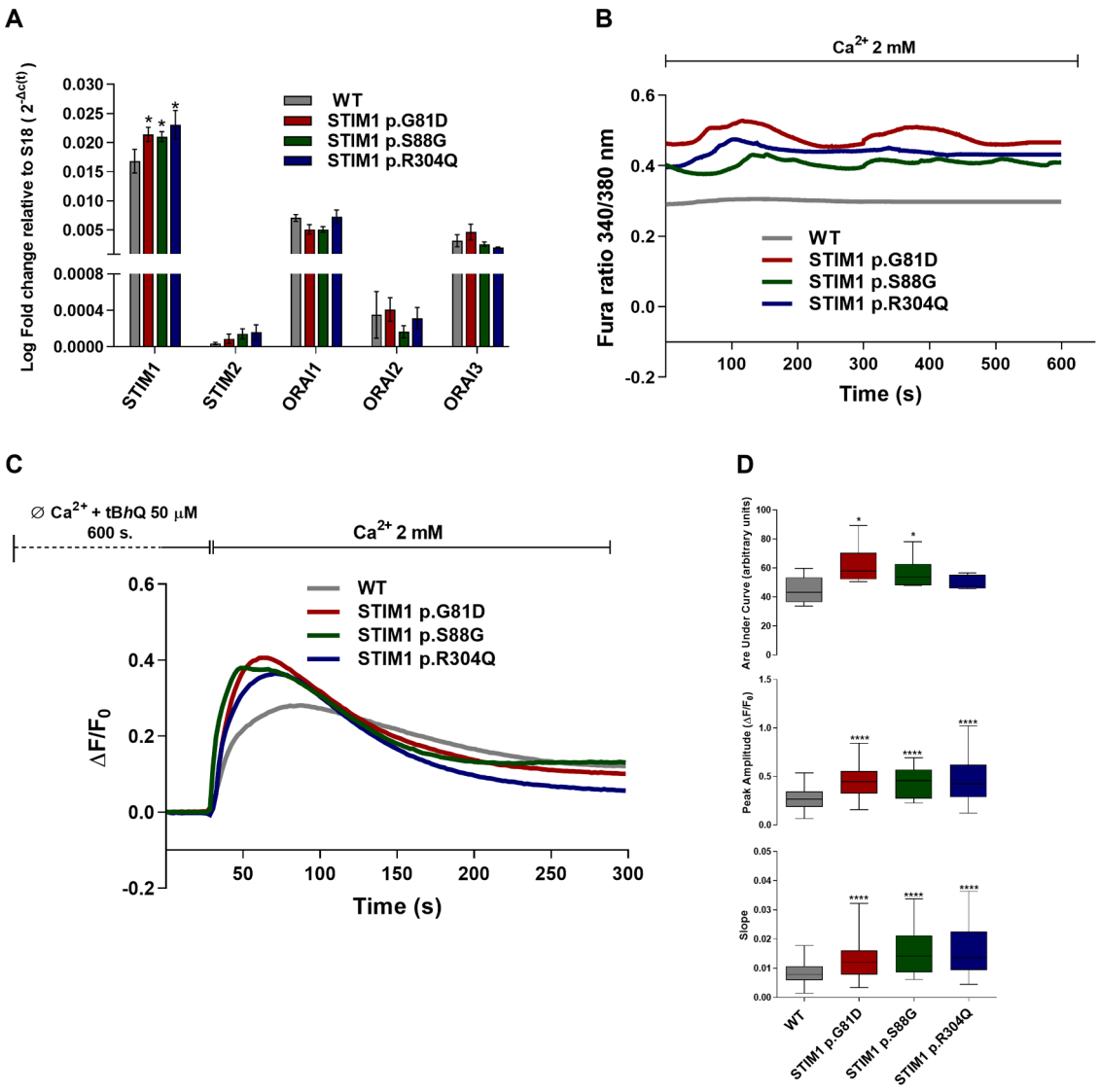

Figure 3. Characterization of Ca^{2+} alterations in patient-derived fibroblasts

(A) RT-PCR analysis of STIM and ORAI gene expressions in patient fibroblasts. Values represent mean ± S.E.M and are expressed as $2^{-\Delta C(t)}$ of genes/S18 of four independent cultures. Unpaired two-tailed Student's t-test. *P= 0.0174 versus wild-type fibroblasts (WT). (**B**) Representative traces of $[Ca^{2+}]_{basal}$ in fibroblasts from TAM patients compared to fibroblasts harbouring wild-type STIM1; (**C**) SOCE triggered by store depletion by *t*BHQ in WT and patient-derived fibroblasts. Average traces of approximately 200 cells from ten separate coverslips performed on 4 separate days. Data are expressed as the change in the 340/380 ratio from the first point measured to the actual illustrated point (ΔF) over the 340/380 ratio of the first point recorded (F_0). All traces are then off-set to zero from graphical reasons. (**D**) Evaluation of area under the curve (AUC), peak amplitude, and slope of the Ca^{2+}-rise in WT and patient-derived fibroblasts. Box and whisker plots show median and IQR of AUC, peak amplitude and slope of the Ca^{2+}-rise. Mann-Whitney U test. AUC *P ≤ 0.042; peak amplitude ****P≤ 0.0001; slope of Ca^{2+-}rise **P= 0.0033, **** P<0.0001 versus WT fibroblasts. AUC was quantified for 270 s (from second 30 to second 300).

the mutations tested led to other gain-of-function features, namely an increased $[Ca^{2+}]_{basal}$ and an increased Ca^{2+} entry upon store depletion. Given the heterologous nature of the HEK model and the non-systematic nature of data reporting for individual families, it would be unwise to correlate the differences between the mutations with any clinical repercussion. In cells in which the mutation was contextualized, *i.e.* fibroblasts, we also observed spontaneous Ca^{2+} oscillations, an observation that parallels our earlier observation in myotubes from a carrier of the p.S97C ORAI1 mutation [41]. Overall, our data support the gain-of-function nature of the mutations which have not been functionally characterized previously (STIM1 p.F108I and p.I115F) and also suggest that the heterologous model is a convenient, ethical, economic and rapid method to evaluate the consequences of new STIM1 and ORAI1 mutations, although it lacks mechanistic insights on the consequence of the mutation, as the readout appears largely similar throughout all tested clones.

We also tested two chemically distinct molecules which have been previously shown to affect wild type SOCE to evaluate whether the mutations might hamper their pharmacological action. All mutations were sensitive to pharmacological inhibition by both agents with two exceptions. First, the p.V138I mutation located on the SAM [14] was differentially affected by CIC-37 and CIC-39. Given our overall data, that shows that the presence of a mutated STIM1 still confers sensitivity to SOCE inhibitors, why this occurs remains to be established. Second, SOCE in ORAI1 p.R304Q-harboring cells seems to be only marginally affected by either of the two novel compounds. An important observation from our work is that CIC-37 and CIC-39 are efficacious in the ORAI1 p.G98S mutation, which has been reported not to be sensitive to the pharmacological inhibition induced by GSK-7975A [31]. These data might therefore suggest that the activity of the different modulators

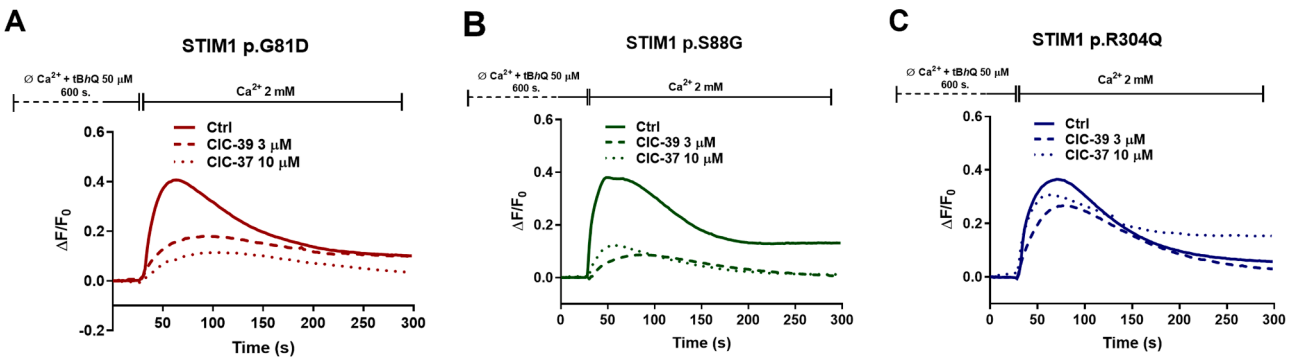

Figure 4. Effect of CIC-39 and CIC-37 on SOCE modulation in patient-derived fibroblast.
Representative traces of SOCE triggered by *t*BHQ store depletion in STIM1 patient-derived fibroblasts in the presence or absence of CIC-37 (10 µM) or CIC-39 (3 µM). Average traces of approximately 100 cells from ten separate coverslips performed on 3 separate days. Data are expressed as the change in the 340/380 ratio from the first point measured to the actual illustrated point (ΔF) over the 340/380 ratio of the first point recorded (F_0). All traces are then off-set to zero from graphical reasons.

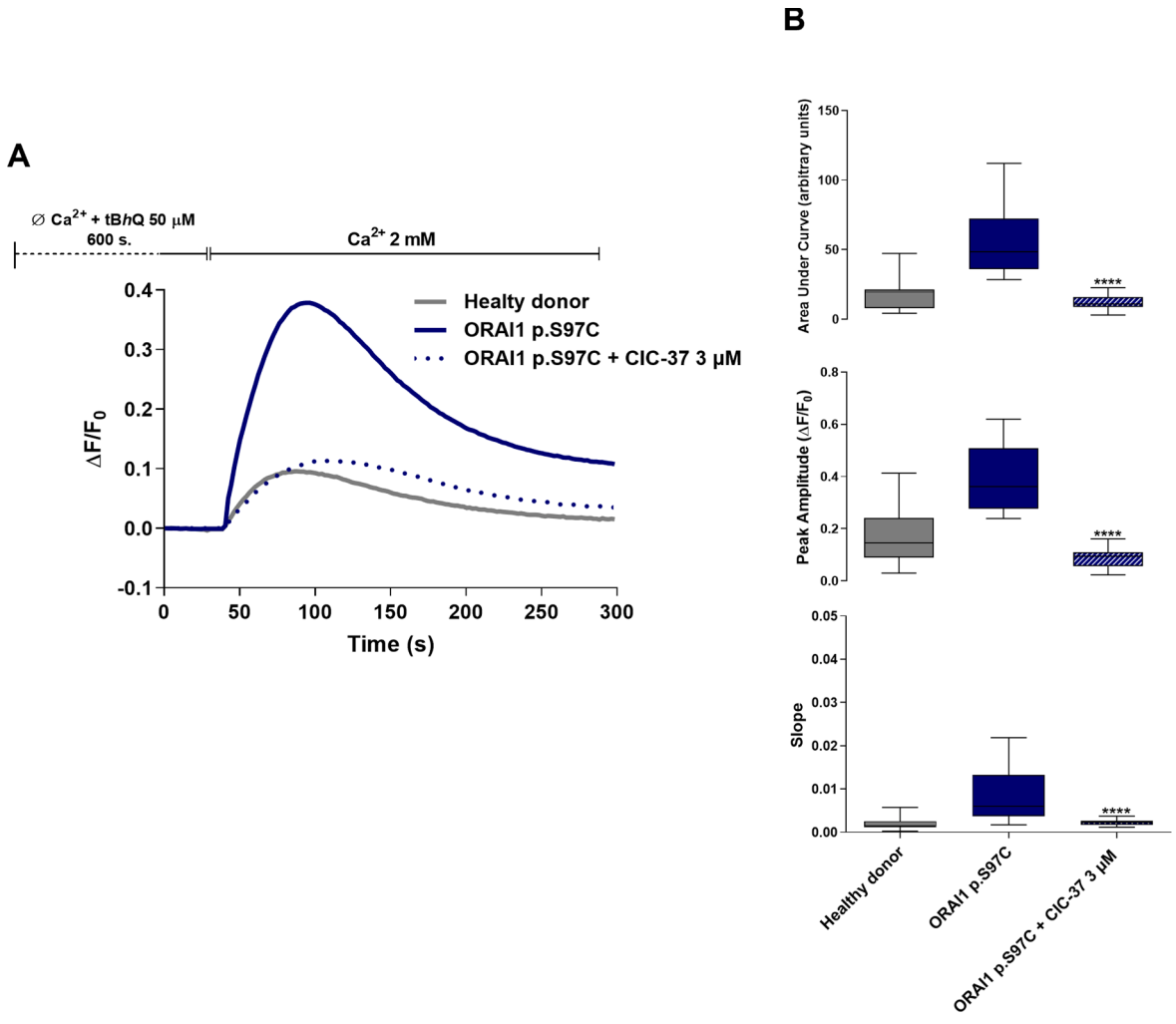

Figure 5. Effect of CIC-37 on SOCE modulation in patient-derived myotubes.
(**A**) Representative traces of SOCE triggered by *t*BHQ store depletion in myotubes from a healthy donor or from a patient bearing the p.S97C ORAI1 mutation in the presence or absence of CIC-37 3 µM. Data are expressed as the change in the 340/380 ratio from the first point measured to the actual illustrated point (ΔF) over the 340/380 ratio of the first point recorded (F_0). All traces are then off-set to zero from graphical reasons.
(**B**) Area under the curve (AUC), peak amplitude, and slope of the Ca^{2+}-rise in presence or absence of CIC-37. Box and whisker plots show median and IQR of AUC, peak amplitude and slope of the Ca^{2+}-rise. Mann-Whitney U test. AUC, peak amplitude and slope of Ca^{2+-}rise **** $P<0.0001$ versus ORAI1 p.S97C mutated myotubes. AUC was quantified for 270 s (from second 30 to second 300).

might be distinct on the different ORAI1 mutants.

In conclusion, our manuscript demonstrates that all SOCE aberrations, with the possible exeption of the R304Q, stemming from STIM1 and ORAI1 mutations are sensitive to the novel SOCE modulators, CIC-37 and CIC-39. Combining this with the acceptable tolerability that SOCE inhibitors have shown in the clinical trials reported so far [21,27], our data, together with the observations by Bulla et al. [31] are promising in envisaging a pharmacological solution in the rehabilitation of TAM patients in the future. If these or other SOCE modulators are brought forward in the clinic, provided that they hold their promise in the mouse models so far developed [47,48], clinical trials should be designed taking into account that some mutations could display a reduced sensitivity to the selected agent.

Credit author statement

Beatrice Riva: Conceptualization, Writing – original draft, Methodology, Investigation, Review and editing

Emanuela Pessolano: Methodology, Investigation, Review and editing

Edoardo Quaglia: Methodology

Celia Cordero-Sanchez: Investigation, Review and editing

Irene P. Bhela: Methodoloy, Resources

Ana Topf: Methodology, Resources

Marta Serafini: Resources, Review and editing

Daniel Cox: Methodology, Resources

Elizabeth Harris: Methodology, Resources

Matteo Garibaldi: Methodology, Resources

Rita Barresi: Resources, Supervision, Review and editing

Tracey Pirali: Resources, Supervision, Review and editing

Armando A. Genazzani: Conceptualization, Supervision, Writing – original draft, Review and editing

Ethics approval and consent to participate

Human fibroblasts collection and use was approved by Newcastle MRC Centre Biobank for Neuromuscular Diseases (19/NE/0028).

Consent for publication

Not applicable.

Author contribution

Conceptualization BR, AAG; Methodology BR, EQ, IPB, MG, AT, DC, EH; Resources TP, MS, IPB, MG, AT, DC, EH, RB; Investigation BR, EP, CCS; Supervision AAG, TP, RB; Writing – original draft BR AAG; writing, review and editing BR, TP, MS, EP, CCS, RB, AAG

Availability of data and materials

All data generated or analysed during this study are included in this published article and its supplementary information files.

Funding

The present study was supported by research funding from the Italian Telethon Foundation to Armando Genazzani (GGP19110).

Declaration of Competing Interest

B.R. is at present an employee of ChemICare Srl although the work was conducted when she was an employee of the Università del Piemonte Orientale. B.R. and T.P. own stocks of ChemICare Srl. ChemIcare Srl is a company that has licensed the rights to CIC-39 and CIC-37 from patents owned by the Università del Piemonte Orientale. All other Authors have no competing interests.

Supplementary materials

Supplementary material associated with this article can be found, in the online version, at doi:10.1016/j.ceca.2022.102605.

References

[1] R.S. Lacruz, S. Feske, Diseases caused by mutations in ORAI1 and STIM1, Ann. N. Y. Acad. Sci. 1356 (2015) 45–79.
[2] J. Böhm, F. Chevessier, C. Koch, et al., Clinical, histological and genetic characterisation of patients with tubular aggregate myopathy caused by mutations in STIM1, J. Med. Genet. 51 (2014) 824–833.
[3] V. Nesin, G. Wiley, M. Kousi, et al., Activating mutations in STIM1 and ORAI1 cause overlapping syndromes of tubular myopathy and congenital miosis, Proc. Natl. Acad. Sci. U. S. A. 111 (2014) 4197–4202.
[4] Y. Endo, S. Noguchi, Y. Hara, et al., Dominant mutations in ORAI1 cause tubular aggregate myopathy with hypocalcemia via constitutive activation of store-operated Ca(2)(+) channels, Hum. Mol. Genet. 24 (2015) 637–648.
[5] H. Stormorken, H. Holmsen, R. Sund, et al., Studies on the haemostatic defect in a complicated syndrome. An inverse Scott syndrome platelet membrane abnormality? J. Thromb. Haemost. 74 (1995) 1244–1251.
[6] L.J. Jiang, X. Zhao, Z.Y. Dou, Q.X. Su, Z.H. Rong, Stormorken syndrome caused by a novel STIM1 mutation: a case report, Front Neurol 12 (2021), 522513.
[7] T. Markello, D. Chen, J.Y. Kwan, et al., York platelet syndrome is a CRAC channelopathy due to gain-of-function mutations in STIM1, Mol. Genet. Metab. 114 (2015) 474–482.
[8] J.W. Putney, A model for receptor-regulated calcium entry, Cell Calcium 7 (1986) 1–12.
[9] M. Prakriya, R. Lewis, Store-operated calcium channels, Physiol. Rev. 95 (2015) 1383. –1346.
[10] V. Barone, V. Del Re, A. Gamberucci, et al., Identification and characterization of three novel mutations in the CASQ1 gene in four patients with tubular aggregate myopathy, Hum. Mutat. 38 (2017) 1761–1773.
[11] J. Böhm, X. Lornage, F. Chevessier, et al., CASQ1 mutations impair calsequestrin polymerization and cause tubular aggregate myopathy, Acta Neuropathol. 135 (2018) 149–151.
[12] J. Böhm, M. Bulla, J.E. Urquhart, et al., ORAI1 mutations with distinct channel gating defects in tubular aggregate nyopathy, Hum. Mutat. 38 (2017) 426–438.
[13] G. Morin, V. Biancalana, A. Echaniz-Laguna, et al., Tubular aggregate myopathy and stormorken syndrome: mutation spectrum and genotype/phenotype correlation, Hum. Mutat. 41 (2020) 17–37.
[14] C. Ticci, D. Cassandrini, A. Rubegni, et al., Expanding the clinical and genetic spectrum of pathogenic variants in STIM1, Muscle Nerve 64 (2021) 567–575.
[15] E. Harris, J. Hudson, J. Marsh, et al., A novel STIM1 mutation at p.340 causes tubular aggregate myopathy with miosis without additional features of Stormorken syndrome, Neuromuscul. Disord. 25 (2015) S289.
[16] M. Fahrner, M. Stadlbauer, M. Muik, et al., A dual mechanism promotes switching of the Stormorken STIM1 R304W mutant into the activated state, Nat. Commun. 9 (2018) 825.
[17] G. Morin, N.O. Bruechle, A.R. Singh, et al., Gain-of-function mutation in STIM1 (p. R304W) Is associated with stormorken syndrome, Hum. Mutat. 35 (2014) 1221–1232.
[18] Study of CM4620 to Reduce the Severity of Pancreatitis Due to Asparaginase. Identifier: NCT04195347. https://clinicaltrials.gov/ct2/show/NCT04195347. Last update November 1, 2021. (Accessed December 20, 2021).
[19] CM4620 injectable emulsion versus supportive care in patients with acute pancreatitis and SIRS. Identifier: NCT03401190. https://clinicaltrials.gov/ct2/show/NCT03401190. Last update: December 7, 2021. (Accessed December 20, 2021).
[20] A PK/PD Study of CM4620-IE in Patients With Acute Pancreatitis. Identifier: NCT03709342. https://clinicaltrials.gov/ct2/show/NCT03709342. Last update: September 19, 2019. (Accessed December 20, 2021).
[21] C. Bruen, J. Miller, J. Wilburn, et al., Auxora for the treatment of patients with acute pancreatitis and accompanying systemic inflammatory response syndrome, Pancreas 50 (2021) 537–543.
[22] A Study of Auxora in Patients With Acute Pancreatitis and Accompanying SIRS (CARPO). Identifier: NCT04681066. https://clinicaltrials.gov/ct2/show/NCT04681066. Last update December 17, 2021. (Accessed December 20, 2021).
[23] A Study of Auxora in Patients With Severe COVID-19 Pneumonia. Identifier: NCT04345614. https://clinicaltrials.gov/ct2/show/NCT04345614. Last update : August 3, 2021. (Accessed December 20, 2021).
[24] A Study of Auxora in Patients With Critical COVID-19 Pneumonia. Identifier : NCT04661540. https://clinicaltrials.gov/ct2/show/NCT04661540. Last update : August 2, 2021. (Accessed December 20, 2021).
[25] J. Miller, C. Bruen, M. Schnaus, et al., Auxora versus standard of care for the treatment of severe or critical COVID-19 pneumonia: results from a randomized controlled trial, Crit. Care 24 (2020) 502.
[26] Safety, Tolerability and Pharmacokinetics of Oral Doses of RP3128 of Rhizen Pharmaceuticals. Identifier: NCT02958982. https://clinicaltrials.gov/ct2/show/NCT02958982. Last update: October 4, 2019. (Accessed December 20, 2021).

[27] P.J Barde, S. Viswanadha, S. Veeraraghavan, S.V. Vakkalanka, A. Nair, A first-in-human study to evaluate the safety, tolerability and pharmacokinetics of RP3128, an oral calcium release-activated calcium (CRAC) channel modulator in healthy volunteers, J. Clin. Pharm. Ther. 46 (2021) 677–687.
[28] A Study of PRCL-02 in Moderate to Severe Chronic Plaque Psoriasis. Identifier: NCT03614078. https://clinicaltrials.gov/ct2/show/NCT03614078. Last update: March 30, 2020. (Accessed December 20, 2021).
[29] Safety and Efficacy Study of RP4010, Patients With Relapsed or Refractory Lymphomas. Identifier: NCT03119467, December 27, 2019 https://clinicaltrials.gov/ct2/show/NCT03119467. Last update:Accessed December 20, 2021.
[30] H. Shawer, K. Norman K, CW. Cheng, et al., ORAI1 Ca^{2+} channel as a therapeutic target in pathological vascular remodelling, Front. Cell. Dev. Biol. 9 (2021), 653812.
[31] M. Bulla, G. Gyimesi, J.H. Kim, et al., ORAI1 channel gating and selectivity is differentially altered by natural mutations in the first or third transmembrane domain, J. Physiol. 597 (2019) 561–582.
[32] L. Waldherr, A. Tiffner, D. Mishra, et al., Blockage of store-operated Ca^{2+} influx by synta66 is mediated by direct inhibition of the Ca^{2+} selective orai1 pore, Cancers 12 (2020) 2876.
[33] NR. Khedkar, NR. Irlapatti, D. Dadke, et al., Discovery of a novel potent and selective calcium release-activated calcium channel inhibitor: 2,6-Difluoro-N-(2′-methyl-3′-(4-methyl-5-oxo-4,5-dihydro-1,3,4-oxadiazol-2-yl)-[1,1′-biphenyl]-4-yl) benzamide. Structure-activity relationship and preclinical characterization, J. Med. Chem. 64 (2021) 17004–17030.
[34] M. Wei, Y. Zhou, A. Sun, et al., Molecular mechanisms underlying inhibition of STIM1-Orai1-mediated Ca^{2+} entry induced by 2-aminoethoxydiphenyl borate, Pflugers Arch. 468 (2016) 2061–2074.
[35] I. Derler, R. Schindl, R. Fritsch, et al., The action of selective CRAC channel blockers is affected by the Orai pore geometry, Cell Calcium 53 (2013) 139–151.
[36] JV. Gerasimenko, O. Gryshchenko, PE. Ferdek, et al., Ca^{2+} release-activated Ca^{2+} channel blockade as a potential tool in antipancreatitis therapy, Proc. Natl. Acad. Sci. U. S. A. 110 (2013) 13186–13191.
[37] H. Schleifer, B. Doleschal, M. Lichtenegger, et al., Novel pyrazole compounds for pharmacological discrimination between receptor-operated and store-operated Ca (2^{+}) entry pathways, Br. J. Pharmacol. 167 (2012) 1712–1722.
[38] B. Riva, A. Griglio, M. Serafini, et al., Pyrtriazoles, a novel class of store-operated calcium entry modulators: discovery, biological profiling, and in vivo proof-of-concept efficacy in acute pancreatitis, J. Med. Chem. 61 (2018) 9756–9783.
[39] S.W. Ng, J. Di Capite, K. Singaravelu, A.B. Parekh, Sustained activation of the tyrosine kinase Syk by antigen in mast cells requires local Ca^{2+} influx through Ca^{2+} release-activated Ca^{2+} channels, J. Biol. Chem. 283 (2008) 31348–31355.
[40] M. Serafini, C. Cordero-Sanchez, R. Di Paola, et al., Store-operated calcium entry (SOCE) as a therapeutic target in acute pancreatitis: discovery and development of drug-like SOCE inhibitor, J. Med. Chem. 63 (2020) 14761–14779.
[41] M. Garibaldi, F. Fattori, B. Riva, et al., A novel gain-of-function mutation in ORAI1 causes late-onset tubular aggregate myopathy and congenital miosis, Clin. Genet. 91 (2016) 780–786.
[42] C. Cordero-Sanchez, B. Riva, S. Reano, et al., A luminal EF-hand mutation in STIM1 in mice causes the clinical hallmarks of tubular aggregate myopathy, Dis. Model. Mech. 3 (2) (2020), 13.
[43] G Grynkiewicz, M Poenie, RY. Tsien, A new generation of Ca^{2+} indicators with greatly improved fluorescence properties, J. Biol. Chem. 260 (1985) 3440–3450.
[44] E. Harris, U. Burki, C. Marini-Bettolo, et al., Complex phenotypes associated with STIM1 mutations in both coiled coil and EF-hand domains, Neuromuscul. Disord. 9 (2017) 861–872.
[45] J. Böhm, M. Bulla, J.E. Urquhart, et al., ORAI1 mutations with distinct channel gating defects in tubular aggregate myopathy, Hum. Mutat. 38 (2017) 426–438.
[46] R. Silva-Rojas, J. Laporte, J. Böhm, STIM1/ORAI1 loss-of-function and gain-of-function mutations inversely impact on SOCE and calcium homeostasis and cause multi-systemic mirror diseases, Front. Physiol. 11 (2020), 604941.
[47] R. Silva-Rojas, S. Treves, H. Jacobs, et al., STIM1 over-activation generates a multi-systemic phenotype affecting the skeletal muscle, spleen, eye, skin, bones and immune system in mice, Hum. Mol. Genet. 28 (2019) 1579–1593.
48 TH. Gamage, G. Gunnes, RH. Lee, STIM1 R304W causes muscle degeneration and impaired platelet activation in mice, Cell Calcium 76 (2018) 87–100.